Chapter V:

Greenish Quartz from the Thunder Bay Amethyst Mine Panorama, Thunder Bay, Ontario, Canada

Laura Baker Hebert and George Rossman

Published as:

L. B. Hebert and G. R. Rossman (2008) Greenish Quartz from the Thunder Bay Amethyst Mine Panorama, Thunder Bay, Ontario, Canada. The Canadian Mineralogist **46**, 61-74, doi: 10.3749/canmin.46.1.000.

Abstract

Naturally occurring greenish quartz found within the context of amethyst-bearing deposits is not simply the result of the exposure of amethyst to thermal bleaching or exposure to the sun. Rather, it can represent a set of distinct color varieties resulting from the changing chemical and thermal nature of the precipitating solution. Greenish quartz occurs at the Thunder Bay Amethyst Mine Panorama (TBAMP), Thunder Bay, Ontario, Canada, in several distinct varieties. Yellowish green quartz and dark green quartz with purple hues occur as loose detritus, and pale greenish gray quartz occurs as part of a color-gradational mineralization sequence involving macrocrystalline quartz of other colors and chalcedony. The TBAMP system contains a number of color varieties of quartz including greenish, amethyst, colorless, and smoky. Spectroscopic, irradiation, and controlled heating studies show that changes in salinity and temperature of the hydrothermal system that produced the TBAMP deposit are reflected in the changing coloration of the quartz. The greenish quartz, especially the greenish gray variety, has increased turbidity and fluid inclusions when compared with the adjacent amethyst. Analysis of different colors on major (r = {10-11}) and minor (z = {01-11}) rhombohedral sectors within the quartz indicates that changes in the growth rate also have influenced color development. As the system evolved, two factors contributed to the color changes: (i) a minor ferric component appears to change position from interstitial to substitutional within specific growth sectors and (ii) the trace element composition of the quartz evolved. The samples from the TBAMP deposit are compared to isolated samples of greenish quartz collected from three

other amethyst-bearing localities: Farm Kos and Farm Rooisand (Namibia), Kalomo-Mapatiqya (Zambia), and Southern Bahia (Brazil). All included similar greenish hues with the exception of the yellowish green variety. Colors within the quartz are consistently correlated with the speciation of hydrous components. Darker green samples incorporate larger amounts of molecular water than either pale greenish gray samples, colorless samples, or amethyst. The appearance of strong hydroxyl peaks in the infrared spectra is limited to amethyst and colorless varieties.

Keywords: amethyst, green quartz, Thunder Bay, Ontario

1. Introduction

The Thunder Bay Amethyst Mine Panorama (TBAMP) deposit is the site of an extinct hydrothermal system that flowed through a fault and led to mineralization primarily by quartz [1]. Although most of the quartz is amethystine, greenish quartz has been found in the TBAMP in several distinct varieties. Yellowish green quartz and dark green quartz with purple hues are found as loose detritus within the TBAMP (originating from outcroppings), and pale greenish gray quartz is found as part of an outcropping color-gradational sequence involving macrocrystalline quartz of other colors, including colorless, smoky gray, and chalcedony (Fig. 1). The color-gradational sequence occurs solely in a localized zone, which may be the site of initial influx of fluids into the fault. Distally, the color of the *in situ* quartz is dominantly dark violet amethyst. In some cases, this dark

violet amethyst, when cut perpendicular to its *c* axis, is found to be composed of alternating sectors of colorless and dark purple quartz.

It is important to understand the origin of the greenish gray color because it is ubiquitously present within a progressive color sequence in quartz. Clues in the chemical and spectroscopic variations within the sequence may provide an increased understanding of the development and persistence of radiation-induced color centers in quartz within the context of changing chemical, thermal, and kinetic factors in a hydrothermal system. The yellowish green and dark green varieties, while not observed *in situ*, will still allow inferences to be made about origins of natural green color in quartz.

2. Background Information

A greenish coloration in synthetic quartz can arise from irradiation of quartz, heating of quartz originally of another color, or from the presence of ferrous iron within the structure [2-5]. However, natural examples of greenish coloration in quartz are rare [6-8], and have not been fully discussed within the context of their environment of formation or in relation to other associated colors of quartz. To initially characterize the greenish color variety, spectroscopic examination of both the greenish and associated color varieties of quartz must be carried out. Additionally, visual observations and spectroscopic analyses of the different color varieties in the TBAMP system should be interpreted specifically in association with radiation exposure and heat-treatment experiments.

In all the samples included in this study, amethyst is consistently associated with the greenish quartz. The violet coloration in amethyst is due to the removal of an electron

by high-energy radiation that results in oxidation of ferric iron within the quartz structure to Fe^{4+} [9]. It has been argued that the ferric iron impurity can be present as either a substitutional or interstitial species, and that its particular structural environment may have an influence on color-center development. In addition to amethyst, smoky quartz was found at the TBAMP associated with the greenish quartz. Commonly characterized by a brownish gray hue, smoky quartz represents another color variety of quartz produced by ionizing radiation. The smoky color center is modeled as Al^{3+} substituting into the Si^{4+} tetrahedral site, with associated charge-balance fulfilled by a nearby positively charged ion (such as Li^{+}) in an interstitial site. Upon irradiation, an electron will migrate away, leaving a "hole center," and the associated charge-compensating cation will migrate away through the structure as well [10]. The source of the ionizing radiation is readily available as ^{40}K within the Archean granitic country-rock surrounding the TBAMP deposit.

McArthur et al. [1] proposed that greenish coloration at TBAMP is heat-induced "bleaching" of amethyst. Heating of quartz can thermally activate color centers and encourage migration of species within the structure. By destroying color centers, heat treatment can selectively eliminate components of coloration associated with exposure to ionizing radiation. We tested this hypothesis by subjecting the amethyst in the TBAMP system to carefully designed heating experiments. Because the presence of molecular H_2O within the quartz structure has been found to be detrimental to the development of certain colors and may allow other colors to emerge instead [11], it is also necessary to examine the incorporation of H_2O in TBAMP quartz.

3. TBAMP Geological Setting and Sample Description

Approximately 1.1×10^9 years ago, the development of the Mid-continent Rift initiated the intrusion of mafic dike swarms [12] followed by faulting in the region of the TBAMP [13]. The hydrothermal vein system utilized by the TBAMP is hosted within an Archean intrusion of granitic rocks located on the boundary between the Quetico and Wawa subprovinces [1]. The amethyst-bearing veins occur within a strike-slip fault, and are part of a chain of amethyst deposits associated with silver and lead-zinc-barite deposits that form along the contact between the Mesoproterozoic Sibley Group and the Archean granite-greenstone assemblage [1]. The timing of events in this region is disputed. Heat derived from the initiation of Keeweenawan rifting and associated intrusions may have mobilized and expelled brines from Sibley Group sediments and driven the fluids parallel to major faults, giving rise to the development of the hydrothermal systems responsible for quartz and ore-deposit mineralization [14]. Alternatively, mineralization may be associated with the formation of the Sibley Basin, wherein diagenetic expulsion of pore waters in conjunction with a thermal anomaly may have contributed to forming the lead-zinc-barite and quartz deposits [1].

The greenish quartz occurs in a range of shades from pale greenish gray to dark translucent green with purple hues to pale greenish yellow, and occurs exclusively in a centralized brecciated zone in the East Pit of the TBAMP, approximately 10 meters in diameter. This zone may have served as the location of initial influx of fluid into the fault. The breccia consists of pebble to small boulder-scale angular fragments of granite, greenstone, laminated chert, and potassium feldspar-rich pegmatite. The brecciation event may have been initiated by hydrofracture, as brecciated fragments tend to be well-sorted

and subangular to subrounded, a consequence of fluid transport [1]. The breccia has been mineralized by quartz in a color sequence that includes the greenish gray coloration. Brecciated pieces are jumbled together, and the mineralized sequence, which nucleated on the breccia surface, has grown outward from that surface, commonly resulting in the abutment of different sequences of quartz. Loose pieces were found consisting of amethyst and greenish gray quartz adjacent to each other, but separated by a millimeter-scale chalcedony horizon. Vein mineralization tens of meters from this zone includes dominantly the color-zoned dark purple amethyst above a thin (2 mm ± 0.5 mm) layer of colorless quartz and dark purple amethyst capped by yellowish white fluid-inclusion-rich quartz. Late-stage amethyst in some areas is capped by dark red hematite flakes. The macrocrystalline varieties of quartz in the mineralization sequence have subparallel directions of growth, with the greatest variations in consistent orientation of the *c* axis found in the early (greenish gray and colorless) sections. Sub-millimeter euhedral grains of pyrite and chalcopyrite are consistently associated with the chalcedony layers.

Samples representative of the color sequence were taken from a single block, 006, from which a vertical section could be selected containing all the color variations in the sequence. Samples were taken from the macrocrystalline sections, focusing on the greenish gray, colorless to brownish gray, and bicolored sections. Detrital samples representative of the dark green and yellowish green varieties were chosen for their internal quality and uniformity of color. Samples characteristic of the dark purple amethyst and common pale purple amethyst were also collected from loose detritus. Most samples were cut so that spectroscopic analyses could be performed with the light polarized to be either parallel or perpendicular to the *c* axis, and others were cut in a plane perpendicular to the *c*

axis, so that sector coloration could be observed. The samples were then doubly polished using alumina polishing paper. For infrared and near-infrared studies, samples were cut to less than 1 mm in thickness; for visible spectroscopic analyses, samples were cut to 2-10 mm in thickness. Polished sections of the collected samples allowed high magnification optical observation of fluid inclusions on the order of 1-5 μm diameter. The greenish gray samples, colorless samples, and greenish gray sectors of the bicolored sections all have similarly poor optical quality, with multiple visible inclusions and cracks and high turbidity. The amethyst sectors of the bicolored sections, and the amethyst found elsewhere in the mine, are all of comparatively high optical quality, with low turbidity. The yellowish green samples are of intermediate optical quality, with less turbidity than the greenish gray samples, but not as clear as the amethyst sections.

4. Descriptions of Samples from Other Localities

We obtained a limited sample set of greenish quartz from other amethyst localities. Samples from the Farm Rooisand (FR), Namibia, include amethyst and pale greenish gray quartz (Fig. 2a). Additionally, colorless varieties occur adjacent to amethyst. There is evidence for the changing state of the crystallizing system, as samples include colorless, high-turbidity generations overlain by pale greenish gray quartz, amethyst generations overlain with pale greenish gray quartz, and greenish gray generations overlain with high-turbidity, colorless generations. FR-3(6) is an example of a colorless vug that appears at the top of an amethyst crystal. FR-3(3) is an example of the greenish gray coloration. FR-3(5) is a section cut perpendicular to the *c* axis that shows an older greenish gray tip

overgrown by a colorless generation of high turbidity. FR-3(2) is a section cut perpendicular to the *c* axis that shows an amethyst inner core, and a greenish gray overgrowth. Samples from Bahia, Brazil (GRR 2350) are uniformly dark green (Fig. 2b), but when cut parallel to the *c* axis, there appear sections of colorless quartz alternating with sections of dark green coloration.

5. Experimental Methods

5. 1.Spectroscopy

Infrared (IR) spectra were obtained at room temperature on doubly polished samples at 2 cm^{-1} resolution for up to 1000 scans using a Nicolet 860 FTIR instrument with a CaF_2 or KBr beam splitter, a liquid-nitrogen-cooled MCT-A detector, and Globar source. Near-infrared (NIR) spectra were obtained on the same instrument, but with an InGaAs detector, a SiO_2 beam splitter, and a visible (W-halogen) light source. A lithium iodate Glan-Foucault prism polarizer (Inrad 703-150) was used to obtain polarized spectra on oriented samples. Visible spectra were obtained at 1 nm resolution for 100 scans with a diode-array spectrometer system consisting of an EG&G PAR detection system with Si and InGaAs diode arrays and Acton triple grating spectrometers, in addition to an Oriel Q-housing tungsten lamp. A subjectively determined sloping baseline correction was applied to define peak positions and to correct for wavelength-dependent scattering effects due to internal defects in the crystal.

5.2.Radiation and thermal experiments

Radiation experiments were performed at room temperature using a ^{137}Cs source, which allows doses of 0.84 Mrads/day. Color change was visually estimated on the basis of comparison with an untreated standard sample.

Heating experiments were performed in air using a Lindberg furnace. The samples were subjected to temperatures from 100 to 500°C in 100°C steps over time intervals of 1 hour between temperature steps. The change in color was visually estimated on the basis of a comparison with an unheated standard sample.

6. Results

6.1.Optical spectroscopy

A background that rises toward shorter wavelengths, attributable to scattering from the internal turbidity of the samples, dominates all optical spectra. The absorption is anisotropic: being more intense if light is polarized parallel to the *c* axis. All the samples have a pale hue, and the absorption bands are superimposed on the scattering curve, with a tail from strong absorption in the ultraviolet. In samples with two colors present, such as the bicolored samples and samples 002, an effort was made to isolate regions of uniform color suitable for spectroscopic analysis, but some interference with other colors was unavoidable.

All greenish gray TBAMP samples are turbid, with low to moderate intensity of color. Absorption spectra consist of a broad band centered at approximately 900 nm, with a weak superimposed band centered at approximately 620 nm defining transmittance at green wavelengths and a further weak band at 520 nm in the perpendicular to *c* polarization (Fig. 3). The spectra of the yellowish green TBAMP samples have a band centered at 710 nm with a sharp increase into the ultraviolet region consistent with transmittance at greenish yellow wavelengths (Fig. 4). The dark green samples from the various localities have almost identical spectra: bands centered at 710 and 930 nm, with a weak band at 540 nm (associated with amethyst coloration) showing greater intensity in the perpendicular to c polarization (Fig. 5). The green color is defined by the transmission window in the 540 nm region. Greenish gray sample FR-3(3) shares the major absorption bands with the dark green samples (Fig. 6): we observed absorption centered at ~940 nm, which has been previously indicated for the interstitial ferrous iron impurity associated with synthetic green quartz (Rossman, 1994). Visible spectra obtained for late-stage dark amethyst samples at TBAMP show only the characteristic absorption bands of amethyst.

The samples were analyzed in the 6000 to 2000 cm^{-1} range to examine contributions from fluid inclusions and structurally bound hydroxyl groups. Quartz IR absorption spectra (Fig. 7) include two types of contributions: broad-band contributions, generally from molecular H_2O (broad-band in the 3440 cm^{-1} region), and sharp peak contributions, from hydroxyl groups (peak at 3585 cm^{-1}, for example).

All samples studied have an anisotropic orientation of hydroxyl groups within the structure, but the samples that contain molecular H_2O show isotropic absorption, which commonly indicates its presence as microscopic or macroscopic fluid inclusions distributed

throughout the structure. Indeed, the greenish gray and colorless varieties at TBAMP contain visible fluid inclusions that were verified by Raman spectroscopy to be mostly H_2O.

The IR spectra for late-stage, dark purple amethyst at TBAMP appear very similar to previously published spectra for amethyst from various localities, with a strong dominance of hydroxyl peaks. The greenish samples, colorless samples, and *both* sectors of the bicolored samples all show greater amounts of H_2O present in the structure as both molecular H_2O and hydroxyl groups. The greenish samples have the greatest H_2O contents relative to the other color varieties, a phenomenon that persists even where differently colored sectors are directly adjacent to one another (Fig. 8).

Figure 9a shows that the relative depth of hue has a correlation with the content of molecular H_2O. The "flat top" spectra in Figure 9a for the Namibian and Brazilian samples suggest that the size and distribution of fluid inclusions may be different in the TBAMP samples. It is apparent in the spectra of samples from all localities that quartz with greenish gray coloration, even when in immediate proximity to other colors, consistently has the highest molecular H_2O content.

6.2.Chemical analysis of TBAMP samples

Chemical analyses of quartz from the TBAMP were performed on the Plasma 54 LA-ICP-MS at Ecole Normale Supérieure de Lyon (Table 1). Sodium is a likely constituent based on its common occurrence in other studies and on the composition of the brine from which the quartz precipitated at TBAMP. Microthermometric fluid-inclusion

analysis by [1] showed that the eutectic temperatures in the initial stages of quartz growth are indicative of a brine in the system $CaCl_2$-NaCl-H_2O, whereas late-stage, high-clarity amethyst was most likely representative of a brine system of $CaCl_2$-NaCl and an iron or zinc salt. The concentration of iron in our samples was not measured, but as it is well understood that the mechanism of amethyst color generation requires iron, we assumed that the quartz in the TBAMP system contains iron.

The samples are heterogeneous on a millimeter scale with regard to their trace-element distribution. All samples contain Ga and S (which is most likely derived from fluid inclusions), and the samples within the color sequence all contain Li, but only the dark green samples (002) contain appreciable Na. It appears that the presence of Ca as a trace constituent is limited to the purple varieties and the darkest green samples. Indeed, the composition of the yellowish green variety would most closely match that of the dark amethyst but for the lack of appreciable Ca. The greenish color is associated with Al in all cases except the yellowish green variety. There is a similarity in coloration between the greenish gray samples and the greenish gray sectors of the bicolored samples, but the chemical analysis reveals the absence of K within the greenish gray samples, perhaps accounting for differing behavior during the heating and radiation experiments.

6.3.Heating experiments on TBAMP samples

Heating can lead to thermal activation of electrons or defect species (vacancies or impurity atoms), resulting in color change. For example, citrine (yellowish quartz) is produced by heating amethyst to 300-500°C, which Stock & Lehmann [15] proposed

causes the iron in the amethyst to precipitate as ferric-iron-oxide clusters. Heating caused some color varieties in our study samples to gradually change color (with color change commencing after reaching 300°C), but others showed only an increase in turbidity, with gradually increasing internal cloudiness indicative of cracks developing through decrepitation of fluid inclusions. Optical observation using a petrographic microscope at high magnification revealed the lack of visible (micron-scale) fluid inclusions in samples after heat treatment. The results are summarized in Table 2.

Heating to temperatures of 500°C did not have an appreciable effect on the height or position of the broad band of molecular H_2O absorption centered at 3440 cm^{-1} for the colorless samples or for the greenish gray samples. Where the larger-scale fluid inclusions rupture during heating (leading to the increase in turbidity observed during the experiments), signs of H_2O remain in the IR spectrum, suggesting that some molecular H_2O is trapped within nanoscale fluid inclusions that do not rupture during heating, owing to the mechanical strength of quartz.

6.4.Radiation experiments on TBAMP samples

The results of the radiation experiments are summarized in Table 2. Samples lower in the color sequence (greenish gray and colorless samples) developed a brownish smoky color with the further darkening and development of purple overtones as exposure increased. Notably, for the colorless sample, the color on the *r* and *z* sectors alternated between brownish smoky and pale purple. This finding emphasizes the existence of different patterns of chemical behavior associated with the major and minor rhombohedral

sectors that manifest themselves as color changes, a phenomenon that becomes more significant further up in the color sequence.

Irradiation of the thermally treated samples provides a way to understand the thermally induced destruction or movement of color centers within the crystals. The lack of development of purple coloration in the greenish samples from the color-gradational sequence is interesting because the other greenish varieties in the system did develop it. More specifically, the most H_2O-rich samples (greenish gray) seem to have the least likelihood of developing a purple color upon exposure to radiation after the heating step.

7. Discussion

In this study, we demonstrate that heating of amethyst from the TBAMP system does not produce the greenish coloration in quartz as a secondary effect, as was originally hypothesized by [1]. Instead, the greenish coloration appears to be intrinsic to the development of the system. The amethyst and smoky coloration in quartz, consistently associated with the greenish varieties in the TBAMP system, are produced by ionizing radiation. Irradiation of the system thus is a major factor in the development of coloration, and the greenish color may be attributable to radiation-induced color centers. It is most likely that the source of radiation was ^{40}K decay to ^{40}Ar, with associated emission of a 1.46 MeV gamma ray. Potassium is abundantly present in the granitic host-rock, and this gamma ray has sufficient energy to penetrate several centimeters into the crystals [16].

7.1.The greenish color in quartz: A radiation-induced color center involving aluminum?

There are brownish gray tones in the greenish gray quartz that may be indicative of the presence of aluminum impurities. Furthermore, the laboratory exposure of the greenish gray samples of the TBAMP suite to ionizing radiation induced yet stronger brownish gray overtones and the development of an optical absorption band centered at 660 nm, which is found in the spectrum of smoky quartz. The trace-element analysis confirms the presence of aluminum in all but one of the greenish varieties. This, and the proximity of the greenish gray quartz to the colorless-to-brownish layer in the color sequence, implies that the greenish gray coloration is possibly another variant of smoky coloration in quartz, caused by the interaction of ionizing radiation with substitutional aluminum and charge-balancing cations.

Both Li^{+} and Al^{3+} (and significant molecular H_2O) are associated with IR bands found in the colorless, greenish gray, dark green, and bicolored (only in the greenish gray sector) sections of the TBAMP sequence and the presence of these elements are confirmed by chemical analysis. The identity of the smoky color center in this system may be that proposed by Maschemeyer et al. [17], who used EPR data to describe a color center composed of a Li-Al "hole" center adjacent to a silicon vacancy (smoky color), whereby the vacancy is generated by the incorporation of H_2O in the Si site. The persistence of the brownish gray coloration within the radiation-treated colorless and greenish gray quartz at room temperature and above (to 300°C) indicates that the identity of the possible contributing "smoky" color center may be associated with a charge-compensating cation other than H^{+}. This is indicated because Al-H color centers are unstable at room temperature owing to the rapid diffusion of the proton within the structure [18]. However,

despite the association of the greenish gray varieties with smoky quartz, we find no definite evidence for any of the specific component bands for smoky quartz: A1, 670 nm; A2, 486 nm; A3, 427 nm; B, 314 nm; and C < 270 nm [6] in the untreated samples.

The dark green samples can be described qualitatively as an overprint of amethyst coloration on a greenish smoky background, resulting in a darkening of the color. The dark green TBAMP samples contain both Al and Ca impurities, which may contribute to the combination of greenish smoky and amethyst components. The heating of TBAMP dark green samples produces citrine (a result similar to the heating of dark purple amethyst), and upon exposure to radiation of the thermally bleached samples, a brownish coloration developed over the citrine.

7.2.The importance of H_2O to the development of greenish color

Rossman [5] observed that the amethyst coloration dominates in nature over the smoky coloration even where the aluminum content exceeds the iron content. There may be a similar phenomenon here, whereby the development of the amethyst color has been inhibited in the natural environment in favor of another color component; in this case, greenish. Aines & Rossman [11] discussed quartz crystals with both amethyst and citrine zones in which molecular H_2O is the dominant species associated with citrine and hydroxyl group is dominant in the amethyst zones. A feature of the dark green quartz is the dominance of molecular H_2O bands in the infrared spectrum. Molecular H_2O contained in these samples has a significant effect on coloration, as irradiation may dissociate it into free radicals, specifically H^0, which could migrate through the structure and allow reaction with

electron hole centers [11, 19]. The amethyst coloration darkened in amethyst sectors upon irradiation in bicolored sample 006-BI, with a simultaneous apparent decrease in the intensity of the broad band for molecular H_2O at 3440 cm^{-1} (measured at the same spot). The dissociation of molecular H_2O into free radicals thus may not have a significant color-dilution effect for amethyst color centers in this system. However, a strongly negative correlation of natural amethyst color with molecular H_2O content is seen in all localities. The amethyst color in the TBAMP bicolored variety of quartz, where there is a strong band due to molecular H_2O, is relatively weak, and hydroxyl peaks dominate the IR spectra of late-stage amethyst, where the amethyst color is the most intense.

In all types of quartz except for amethyst (later-stage distal generation in the TBAMP suite), the IR spectra show both structurally bound H_2O and molecular H_2O that can be interpreted as fluid inclusions. The greenish gray samples, dark green samples, and the yellowish green samples all exhibit IR spectra that are dominated by the presence of the broad peak due to molecular H_2O. The presence of molecular H_2O is not a distinguishing factor among the three "types" of greenish quartz, but rather it is the relative amount of H_2O. For all localities, the dark green samples have higher contents of H_2O than the paler green varieties. The increase in turbidity upon heating of the yellowish green samples is not as strong as with the greenish gray samples. The persistence of the molecular H_2O bands during the heating experiments suggests that even though the macro- to micro-scale fluid inclusions rupture during heating, leading to an increase in turbidity, molecular H_2O is trapped within nano-scale fluid inclusions that do not rupture during heating, owing to the mechanical strength of quartz. Perhaps there is an increased distribution of fluid

inclusions as nano-inclusions within the yellowish green quartz compared with the greenish gray quartz.

The appearance of truncated molecular H_2O bands in the Namibian and Brazilian samples (Fig. 9a) does not appear in the TBAMP samples. This truncation may have to do with the size and distribution of fluid inclusions within the quartz structure. Because of their size, and possibly because of a more uniform distribution, nano-inclusions would be much less prone to produce truncated H_2O bands in the infrared when compared to macro-inclusions. Along with the results of the heating experiments, this argument leads us to assert that the fluid-inclusion population within the TBAMP quartz may include a significant nano-inclusion subset, but that the presence of nano-scale inclusions is not a requirement for the development of the greenish coloration. It may, however, allow some insights about the conditions of crystallization of quartz in the TBAMP system.

7.3.The role of iron in the development of color

The yellowish green quartz of the TBAMP suite qualitatively shows no brownish smoky component, and further exposure to ionizing radiation has no affect on coloration. The trace-elements present in the yellowish green type are different from the other types of greenish quartz. In particular, the yellowish green quartz contains K, but no Al, Li, Na, or Ca. This agrees with the lack of observable brownish coloration (due to Al, or Li and Al). The presence of ferrous iron in the yellowish green quartz would inhibit the generation of violet tones upon exposure to radiation of the original sample. An explanation put forth for the strong greenish coloration of a form of synthetic quartz ("prasiolite") has been the

reduction of an interstitial ferric iron impurity, which migrates to form ferrous iron in an interstitial channel site characterized by a distorted octahedral symmetry [2]. A transmission window defined by an absorption band centered at 741 nm [20] arises from interstitial Fe^{2+} [21]. A weak absorption can be seen at 950 nm for the yellowish green variety, another band position associated with the interstitial ferrous iron impurity in synthetic green quartz [5]. In addition, the color change upon heating is different than that seen for the other greenish varieties. For the early-stage greenish gray samples, heating produces colorless crystals with increased turbidity, and exposure to radiation produces smoky coloration, both demonstrating the relative lack of iron. In contrast, heating of the yellowish green samples produces strongly yellow citrine, a color that is due to the precipitation of iron oxide clusters in the quartz structure. Cohen & Hassan [3] argued that only interstitial iron is a candidate for precipitation of the clusters as a new phase, and heating in an oxidizing environment can result in the change in oxidation state of the iron from ferrous to ferric. Interestingly, when a *thermally bleached* sample of the yellowish green quartz is subsequently exposed to radiation, a faint purplish color is developed, confirming the presence of ferric iron in the thermally produced citrine (the ferric iron would be a likely precursor to amethyst coloration during subsequent irradiation).

In addition to the yellowish green samples, the amethyst sectors of the TBAMP bicolored generation, the greenish gray sectors of the bicolored generation, the dark green TBAMP samples, and some of the TBAMP dark purple amethyst changed color to citrine when heated. We find some evidence for absorption bands associated with interstitial ferrous iron (at about 950 nm) in the dark green samples and in the Namibian greenish gray

samples. The dark greenish coloration could be indicative of the oxidation state of the formative environment. These materials thus also may contain interstitial iron.

We observed Brazil twinning and biaxial optics on greenish gray sectors in a bicolored sample from the TBAMP suite, but because of sample imperfections, it was difficult to verify a persistence of this phenomenon throughout the TBAMP section. In "ametrine," a naturally occurring bicolored variety of quartz that exhibits amethyst and citrine coloration on the *r* and *z* sectors, respectively, amethyst is normally associated with polysynthetic (Brazil) twinning, which is usually restricted to the major rhombohedral sector *r*. Cohen & Hassan [3] noted that with X-irradiation, synthetic, ferric-iron-doped quartz developed a smoky amethyst color on the *r* sectors and only smoky coloration on the *z* sectors. They also observed that the amethyst-colored regions are biaxial and the dominantly smoky sectors are uniaxial. The presence of polysynthetic twinning has been interpreted as a response by the crystal to strain initiated by the interstitial incorporation of ferric iron in channels perpendicular to the major rhombohedral face, a phenomenon which is presumed to be the precursor to the development of amethyst color [22, 23].

The absence of ferrous iron absorption bands in the greenish gray TBAMP quartz, and the existence of the biaxial character of the greenish gray sectors, may indicate that primarily ferric iron may be present in the structure, though not enough to influence color development when compared to Al impurities. Alternatively, the higher molecular H_2O content in the greenish gray zones could discourage development of the amethyst coloration. Irradiation of the greenish gray sectors produces no change in color. Though qualitatively identical in color, there is an inherent difference between the early-generation greenish gray quartz in the TBAMP suite and the greenish gray variety that appears in the

bicolored generation. The early samples become more turbid and colorless when heated, whereas the bicolored greenish gray samples change to citrine. This may be indicative of the introduction of significant amounts of iron into the system as precipitation of quartz commenced, without an observable qualitative effect on the greenish gray coloration. The biaxial character of the originally greenish gray sectors persists through heating, suggesting that ferric iron remains in an interstitial location within the structure.

7.4.Color as an indicator of the dynamic state of the early TBAMP system

The kinetics of quartz formation has an impact on the generation of color. The formation of bicolored synthetic "ametrine" was evaluated [24] in terms of critical rates of growth of the rhombohedral faces *r* and *z*. As the growth rate increases, the intensity of the amethyst color in both sectors increases, and then the intensity of coloration of the major rhombohedral faces, *r*, decreases relative to *z* as the amethyst is increasingly replaced by citrine [24]. This analysis may define a region that is relevant to the transitional bicolored type of quartz in the TBAMP suite. Major rhombohedral sectors, in both the synthetic cases [24], and perhaps in the bicolored quartz generation at the TBAMP, contain polysynthetic twinning according to the Brazil law.

Crystals of synthetic quartz will incorporate greater amounts of H_2O at higher growth-rates, and the production of flawless synthetic amethyst requires lower growth-rates [25]. Indeed, a negative correlation between content of molecular H_2O and intensity of amethyst color (measured by comparative peak intensity) has been demonstrated in natural "ametrine" [26] and seems to apply in the TBAMP system as well. In the TBAMP

sequence, the highest growth-rates may have existed in the earliest generations of quartz, exclusively greenish gray in color, where the greatest amount of molecular H_2O is found. The presence of an OH band at 3543 cm^{-1} may indicate the formation of a new OH^- defect in the quartz structure due to the influence of a high growth-rate [27]. Colorless sample 006-C has an OH band centered at 3530 cm^{-1} (Fig. 9b, I). During evolution of the system, growth rates decreased, as indicated by the slightly lower contents of molecular H_2O and the presence of very pale amethyst forming on the minor rhombohedral sectors. Finally, the amethyst color dominates, and H_2O is dominantly present as OH groups, possibly indicating the lowest growth-rates. Balitsky et al. [24] described these growth rates to be on the order of 0.3-0.8 mm/day for synthetic quartz.

In the bicolored generation, we contend that ferric iron is present dominantly in substitutional sites (with a minor interstitial component) in the amethyst sectors, and interstitially in the greenish gray sectors. The amethyst sectors in the bicolored section do not seem to exhibit Brazil-law twinning. Ferric iron in a substitutional site should not produce substantial distortion of the structure, and would be consistent with the mechanism understood to lead to color generation in amethyst. Another possibility is that the amethyst sectors of the bicolored section contain a low enough ferric iron content as to not produce significant distortion of the structure, or that only minor amounts of ferric iron are present interstitially.

An additional consideration for the growth of flawless synthetic amethyst is that it requires a Na-free solution [25]. The dominant hydrous component is hydroxyl in a Na-free solution; when Na is included in the solution, additional assimilation of molecular H_2O occurs [28]. This analysis is applicable to the TBAMP system, where salinity drops as the

hydrothermal system persists, supposedly because of progressive mixing of the basinal brine with a meteoric H_2O component [1]. Measurements of the final melting temperatures of the fluid inclusions conducted by McArthur et al. [1] indicate that the TBAMP system experienced a decrease in salinity as the crystals grew, such that the earlier greenish gray generation had a relatively high salinity (approximately 20 equiv. wt. % NaCl) and that the dark amethyst generation had a very low salinity. It is apparent that the evolution of the system from quartz precipitation at a high growth-rate with high amounts of incorporated molecular water and high salinity, to quartz precipitation at a low-growth rate with lower amounts of molecular H_2O and low salinity, contributed to the gradual appearance of amethyst in the sequence. It is significant to conclude that the source of the greenish coloration is definitely not thermal bleaching of amethyst in this system, as previously thought. Indeed, the amethyst color does not begin to fade until temperatures of 300°C are reached, well above the approximately 145°C attained by hydrothermal heating in the TBAMP system.

8. Conclusions

(1) The evolution of color in a particular zone of the TBAMP system allows an examination of the chemical and kinetic factors acting during the early stages of quartz precipitation in the hydrothermal system. Interpretation of the color variations in quartz as environmental indicators stresses the importance of viewing color as a consequence of a system.

(2) The TBAMP quartz deposit, an economical source of dark purple amethyst, has a localized zone, interpreted as an area of initial hydrothermal influx that exhibits a consistent color-gradational mineralization sequence of quartz. This sequence includes naturally occurring greenish gray quartz.

(3) We present a comprehensive series of spectroscopic analyses of the quartz color sequence, supplemented by additional analyses of a limited sample set from similar amethyst-bearing localities worldwide, noting the importance of incorporation of water as hydroxyl and molecular species on color development.

(4) We conclude that the greenish gray coloration is not a secondary result of heating of pre-existing amethyst, but another radiation-induced color variant, which developed its particular color as a result of specific chemical constituents, exposure to radiation, and incorporation of molecular water both as nano-scale and micro- to macro-scale inclusions.

(5) We also conclude that interpretation of color is an important factor in deriving the changing state of early stages of this system, as we use our data to confirm that the hydrothermal system experienced a gradual decrease in salinity and quartz growth rate as deposition proceeded.

Acknowledgments

The authors gratefully acknowledge Stephen Kissin (Lakehead University) for providing the initial sample that led to this project and for his helpful comments and invaluable support during the field stages of the project. We acknowledge Steve and Lorna Lukinuk of TBAMP for their hospitality and for permission to sample in the mine. G.

Niedermayr (Vienna) is thanked for providing the Namibian and Zambian samples. Additional thanks go to Elizabeth Johnson and to Elizabeth Miura Boyd for discussion and assistance with analyses and Francis Albarède (Lyon) for LA-ICP-MS analyses. Funding from NSF (USA) grant EAR-0337816 and the White Rose Foundation are especially appreciated.

References

[1] J. R. McArthur et al. (1993) Stable-isotope, fluid inclusion, and mineralogical studies relating to the genesis of amethyst, Thunder Bay Amethyst Mine, Ontario. Canadian Journal of Earth Sciences **30**, 1955-1969.

[2] G. Lehmann and H. Bambauer (1973) Quarzkristalle und ihre Farben. Angew. Chem. **85**, 281-289; Quartz crystals and their colors. Angew. Chem. Int'l Edn. **12**, 283-291.

[3] A. J. Cohen and F. Hassan (1974) Ferrous and ferric ions in synthetic alpha-quartz and natural amethyst. American Mineralogist **59**, 719-728.

[4] E. Neumann and K. Schmetzer (1984) Mechanism of thermal conversion of colour and colour centres by heat treatment of amethyst. N. Jb. Miner. Mh. **6**, 272-282.

[5] G. R. Rossman (1994) Colored Varieties of the Silica Minerals. In P.J. Heaney, C.T. Prewitt, G.V. Gibbs (eds.), Reviews in Mineralogy, Mineralogical Society of America, Washington, 1994, p. 433.

[6] K. Nassau and B. E. Prescott (1977) A unique green quartz. American Mineralogist **62**, 589-590.

[7] T. R. Paradise (1982) The natural formation and occurrence of green quartz. Gems and Gemmology **18**, 39-42.

[8] A. N. Platonov et al. (1992) Natural prasiolite from Lower Silesia, Poland. Z. Dt. Gemmol. Ges. **41**, 21-27.

[9] R. T. Cox (1977) Optical absorption of the d^4 ion Fe^{4+} in pleochroic amethyst quartz. Journal of Physics, C: Solid State Physics **10**, 4631-4643.

[10] J. A. Weil (1975) The aluminum centers in alpha-quartz. Radiat. Eff. **26**, 261-265.

[11] R. D. Aines and G. R. Rossman (1986) Relationships between radiation damage and trace water in zircon, quartz, and topaz. American Mineralogist **71**, 1186-1986.

[12] P. C. Thurston (1991) Chapter 13. In P.C.Thurston, H.R. Williams, R.H. Sutcliffe, G.M. Stott (eds.), Geology of Ontario. Ontario Geological Survey, Special Volume 4, Part 2, 1991.

[13] H. R. Williams (1991) Chapter 25. In P.C.Thurston, H.R. Williams, R.H. Sutcliffe, G.M. Stott (eds.), Geology of Ontario. Ontario Geological Survey, Special Volume 4, Part 2, 1991.

[14] S. A. Kissin and R. L. Sherlock (1989) Geoscience Research Grant program, Summary of Research 1988-1989, Ontario Geological Survey Miscellaneous Paper **143**, 33-41.

[15] H. D. Stock and G. Lehmann (1977) Phenomena associated with diffusion of trivalent iron in amethyst quartz. J. Phys. Chem. Solids **38**, 243-246.

[16] I. M Reinitz and G. R. Rossman (1988) Role of natural radiation in tourmaline coloration. American Mineralogist **73**, 822-825.

[17] D. Maschemeyer et al. (1980) Two modified smoky quartz centeres in natural citrine. Phys. Chem. Mineral. **6**, 145-146.

[18] J. H. Mackey (1963) An EPR study of impurity related colour centres in aluminum-doped quartz. J. Chem. Phys. **39**, 74-83.

[19] A. M. Hofmeister and G. R. Rossman (1985) A model for the irradiative coloration of smoky feldspar and the inhibiting influence of water. Phys. Chem. Mineral. **12**, 324-332.

[20] H. Rose and J. Lietz (1954) Ein grun verfarbbarer Amethyst. Naturwiss **41**, 448.

[21] G. Lehmann (1967) Farbzentren des Eisens als Ursache der Farbe von Amethyst. Zeit Naturforsch. **22a**, 2080-2086.

[22] A. C. McLaren and D. R. Pitkethly (1982) The twinning microstructure and growth of amethyst quartz. Phys. Chem. Min. **8**, 128-135.

[23] A. J. Cohen (1989) New data on the cause of smoky and amethystine color in quartz. The Mineralogical Record **20**, 365-367.

[24] V. S. Balitsky et al. (2000) Industrial growth, morphology, and some properties of Bi-colored amethyst-citrine quartz (ametrine). Journal of Crystal Growth **212**, 255-260.

[25] V. S. Balitsky (1977) Growth of large amethyst crystals from hydrothermal fluoride solutions. Journal of Crystal Growth **41**, 100-102.

[26] R. D. Aines and G. R. Rossman (1984) Water in minerals? A peak in the infrared. Journal of Geophysical Research **89**, 4059-4071.

[27] Personal communication, V. S. Balitsky (2003)

[28] R. D. Aines et al. (1984) Hydrogen speciation in synthetic quartz. Phys. Chem. Minerals **11**, 204-212.

Figure Captions

Figure 1: Block 006. The color sequence containing the greenish quartz is nucleated on brecciated fragments and consists of (1) reddish chalcedony, (2) macrocrystalline quartz grading from colorless to greenish gray over 2.0 cm ± 0.5cm, (3) a fine (0.5 cm ± 0.2 cm) layer of white chalcedony, (4) macrocrystalline quartz grading from colorless to brownish gray over 2.0 cm ± 1.0 cm, (5) an 8.0 cm ± 3.0 cm "bicolored" generation of pale amethyst and greenish gray quartz color-zoned on minor and major rhombohedral sectors, respectively, and finally, (6) dark purple amethyst with sectors color-zoned to colorless and dark violet.

Figure 2: Greenish samples: (a) Namibian greenish gray sample GRR 2477(1); (b) Brazil dark green samples GRR 2350 (1), and GRR 2350 (2).

Figure 3: Optical spectrum of greenish gray TBAMP sample 006-G showing a band centered at 620 nm. There is a weak band at 520 nm visible in the perpendicular to c polarization direction. The spectra, normalized to 1.0 mm thickness, show a significant increase in scattering from long to short wavelengths.

Figure 4: Unpolarized optical spectrum of yellowish green sample 001 that shows a broad, weak band at 710 nm in addition to a sharp increase into the ultraviolet region consistent with transmission at greenish yellow wavelengths. Plotted at 10.17 mm thick.

Figure 5: Polarized spectra covering the visible and near-infrared regions for dark green sample GRR 2350. Broad bands centered at 710, 930, and 1140 nm with transmittance at 547 nm are correlated with the greenish coloration of the sample.

Figure 6: Spectrum for greenish gray sample FR-3(3) showing broad bands at 710 and ~940 nm similar to the dark green samples. The absorption centered at ~940 nm has been previously indicated for the interstitial ferrous iron impurity associated with synthetic green quartz (Rossman, 1994).

Figure 7: Polarized IR spectra of TBAMP samples 002 (Top: dark green quartz), 001 (Center: yellowish green quartz), and 003 (Bottom: amethyst quartz) demonstrating the broad molecular water band intensity in the greenish samples contrasted with the hydroxyl (OH) peaks dominating the spectrum of the amethyst sample. All spectra are normalized to 1.0 mm thickness and vertically offset for clarity. Solid line: E parallel c; dashed line: E perpendicular c.

Figure 8: IR spectra of different color varieties of TBAMP sample 006 (see Figure 1 for reference) polarized E⊥c. Greenish gray is sample 006-G; colorless is sample 006-C; bicolored quartz is sample 006-BI represented by both a greenish gray sector and an

amethyst sector. All spectra are normalized to 1.0 mm thickness and are offset vertically for clarity. It can be seen qualitatively that the greenish samples have the greatest H_2O contents relative to the other color varieties, even in the case of the bicolored generation when the sectors are adjacent to one another.

Figure 9: IR spectra of different color varieties of Farm Rooisand and Brazil samples polarized E⊥c. All spectra are normalized to 1.0 mm thickness: (a) A comparison of greenish colored samples: I: TBAMP sample 002 (dark green); II: TBAMP sample 001 (yellow green); III: Brazilian sample GRR 2350 (dark green); IV: Namibian sample FR-3 (5) (greenish gray); V (dashed): Namibian sample FR-3(3) (greenish gray). The relative depth of hue has a correlation with the content of molecular H_2O. (b) A comparison of colorless samples: I: TBAMP sample 006-C-3; II: Brazilian sample GRR 2350; III (dashed): Namibian sample FR-3(6); IV: Namibian sample FR-3(5). The colorless samples have qualitatively significant H_2O content, but in comparison with the greenish gray samples in (a), there is an increasing resolution of hydroxyl peaks (labeled) superimposed over the broad band at 3400 cm^{-1}.

Figure 1.

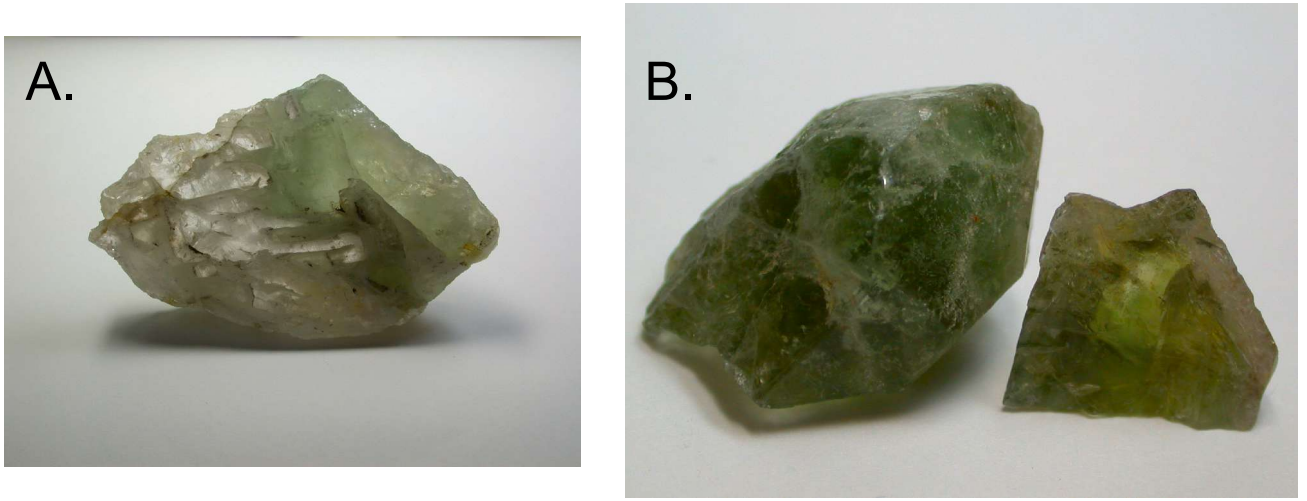

Figure 2.

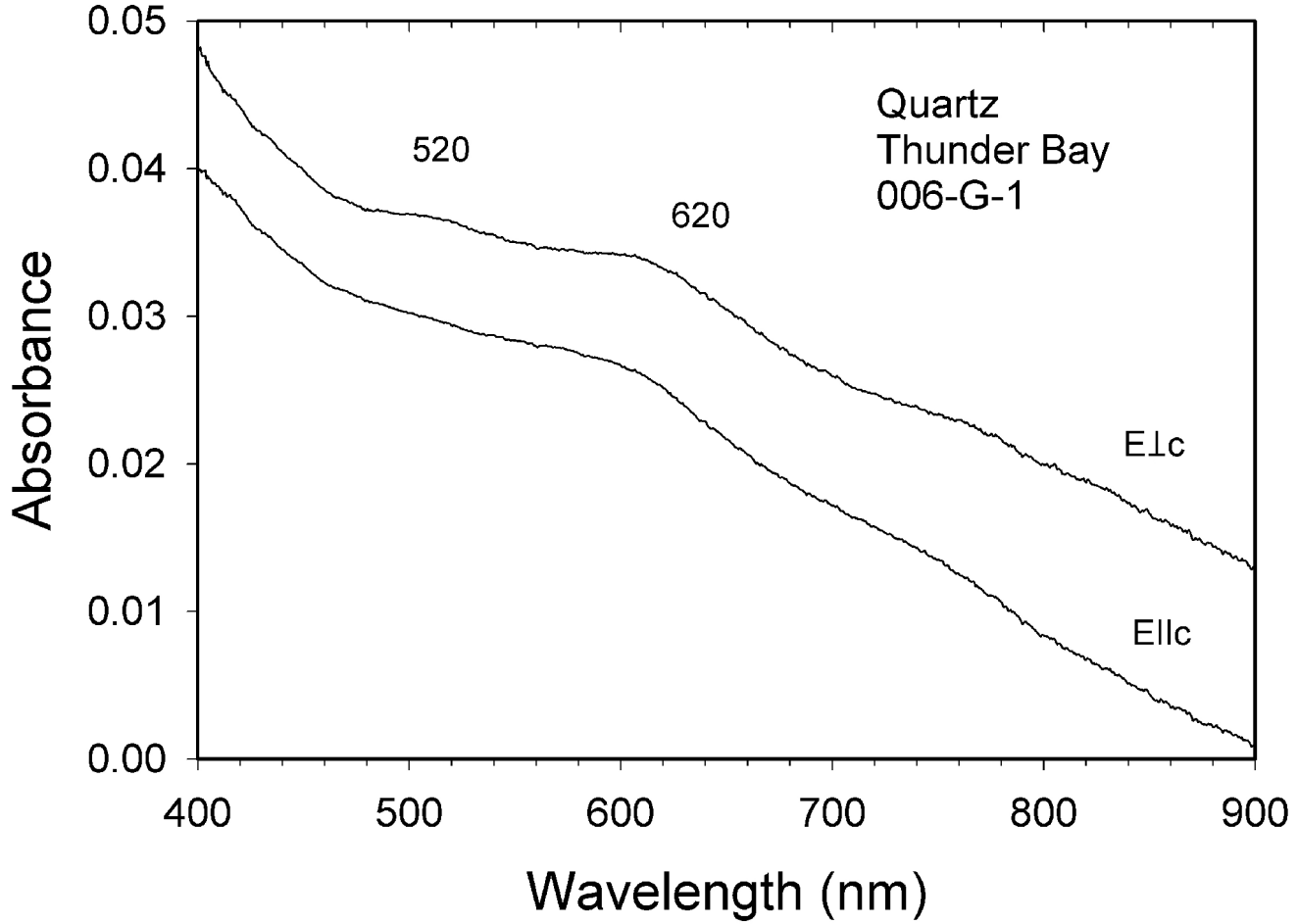
0.05
0.04
0.03
0.02
0.01
0.00
Absorbance
400
500
600
700
800
900
Wavelength (nm)
520
620
Quartz
Thunder Bay
006-G-1
E⊥c
E||c

Figure 3.

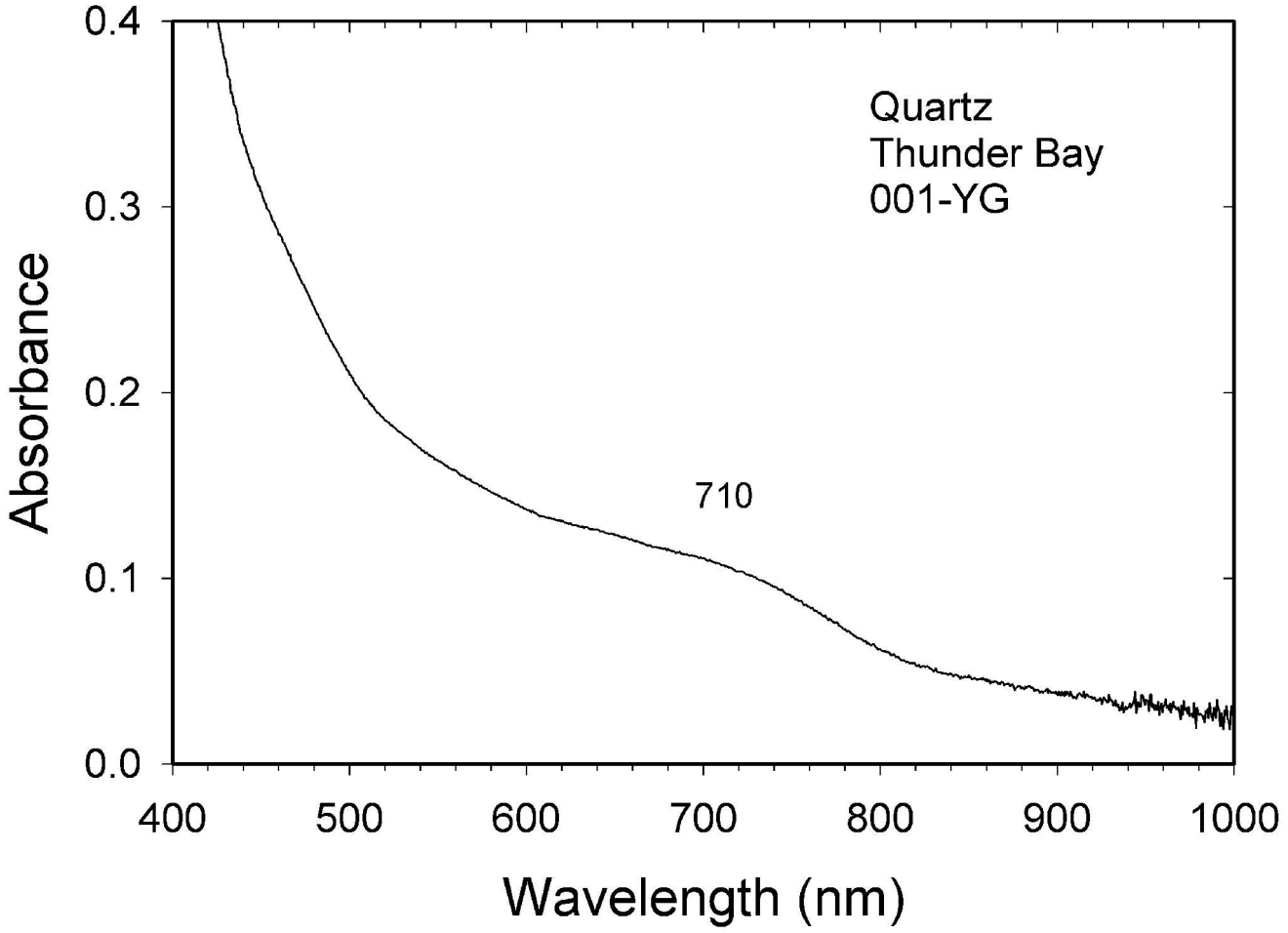
Quartz
Thunder Bay
001-YG
710
Absorbance
0.0
0.1
0.2
0.3
0.4
400
500
600
700
800
900
1000
Wavelength (nm)

Figure 4.

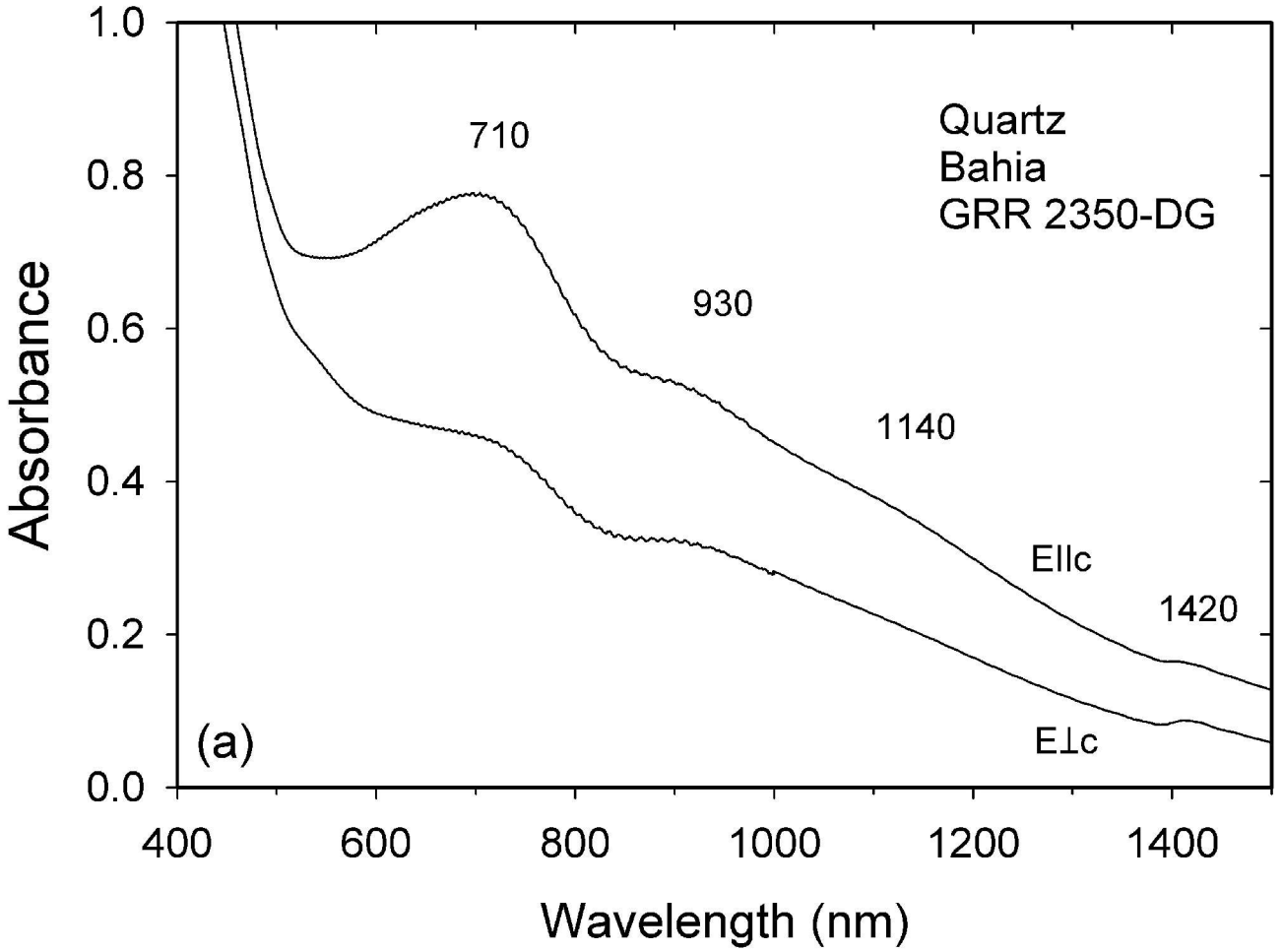
1.0
0.8
0.6
0.4
0.2
0.0
Absorbance
400
600
800
1000
1200
1400
Wavelength (nm)
710
930
1140
1420
Quartz
Bahia
GRR 2350-DG
Ellc
E⊥c
(a)

Figure 5.

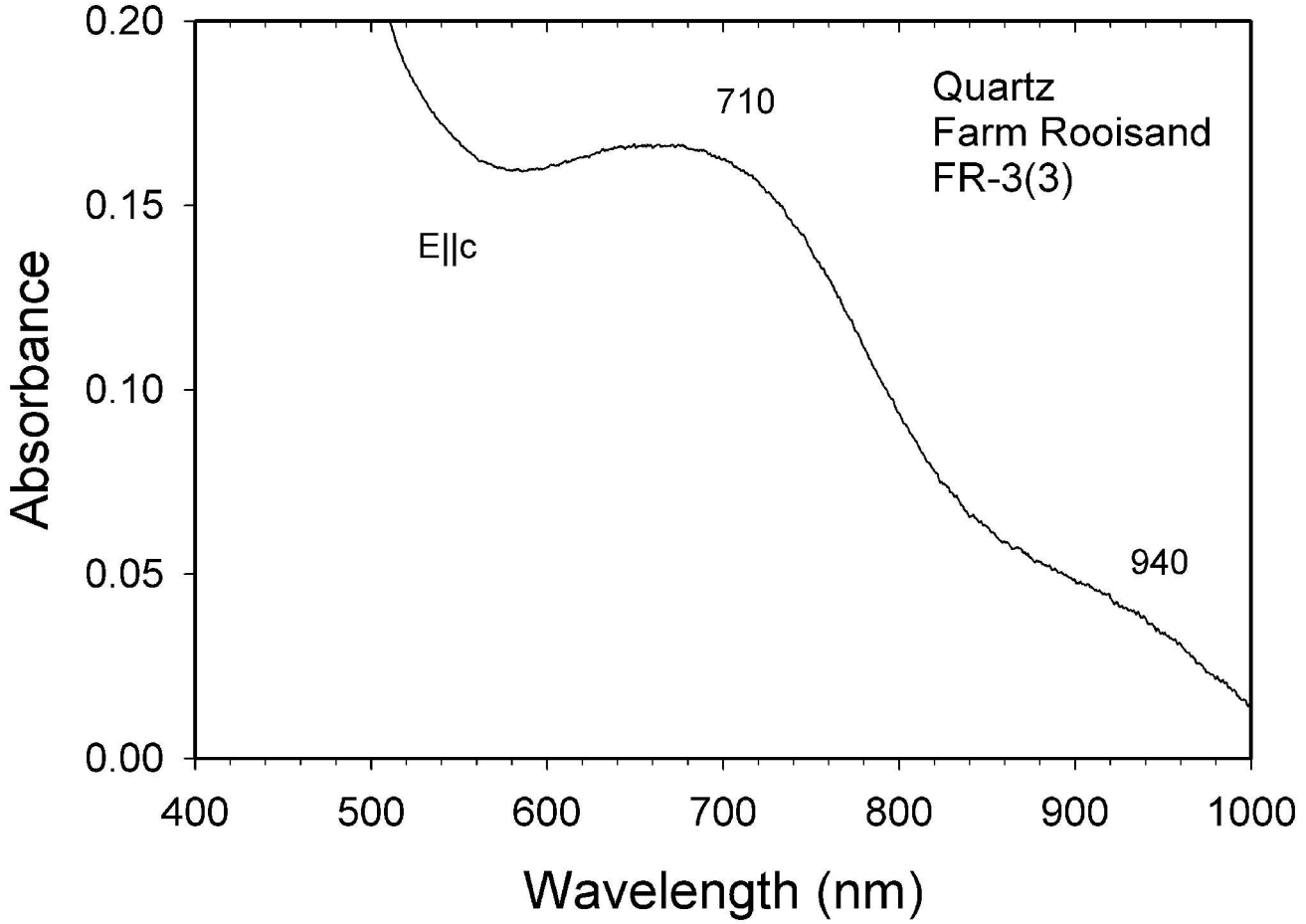
0.20
0.15
0.10
0.05
0.00
Absorbance
400
500
600
700
800
900
1000
Wavelength (nm)
710
940
E||c
Quartz
Farm Rooisand
FR-3(3)

Figure 6.

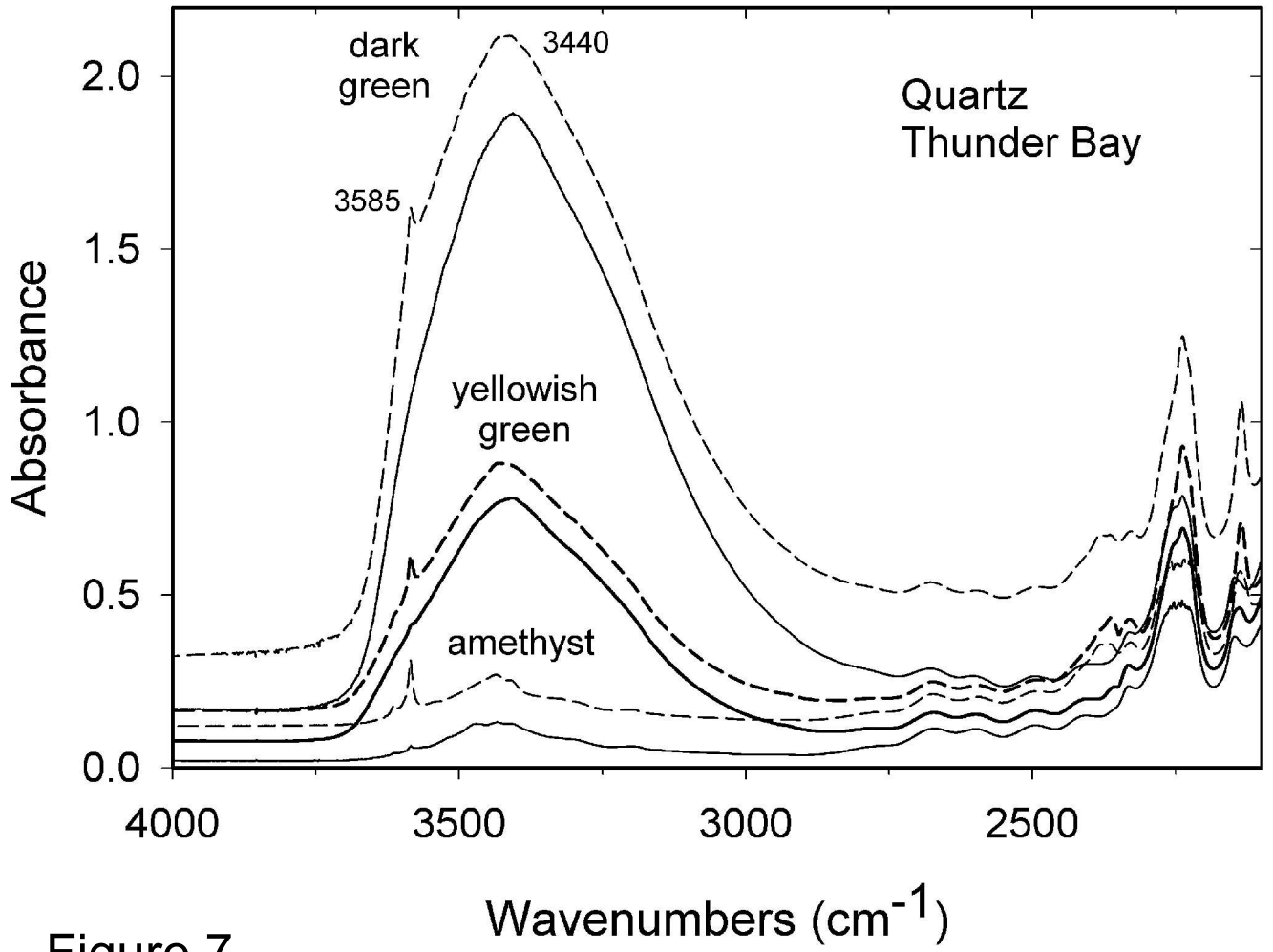
dark
green
3440
3585
Quartz
Thunder Bay
yellowish
green
amethyst
Absorbance
2.0
1.5
1.0
0.5
0.0
4000
3500
3000
2500
Wavenumbers (cm-1)

Figure 7.

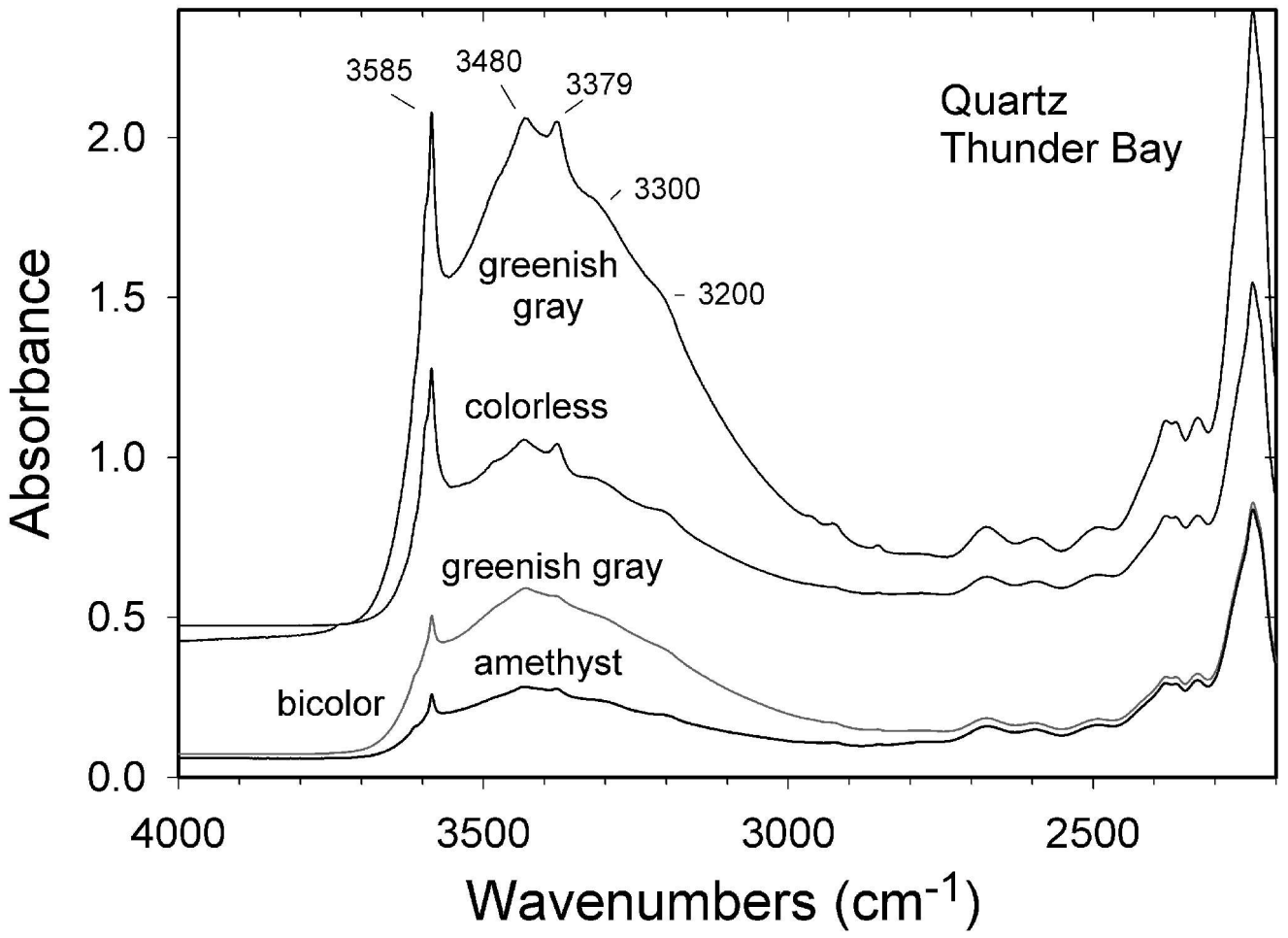
Quartz
Thunder Bay
3585
3480
3379
3300
3200
greenish
gray
colorless
greenish gray
amethyst
bicolor
Absorbance
2.0
1.5
1.0
0.5
0.0
4000
3500
3000
2500
Wavenumbers (cm-1)

Figure 8.

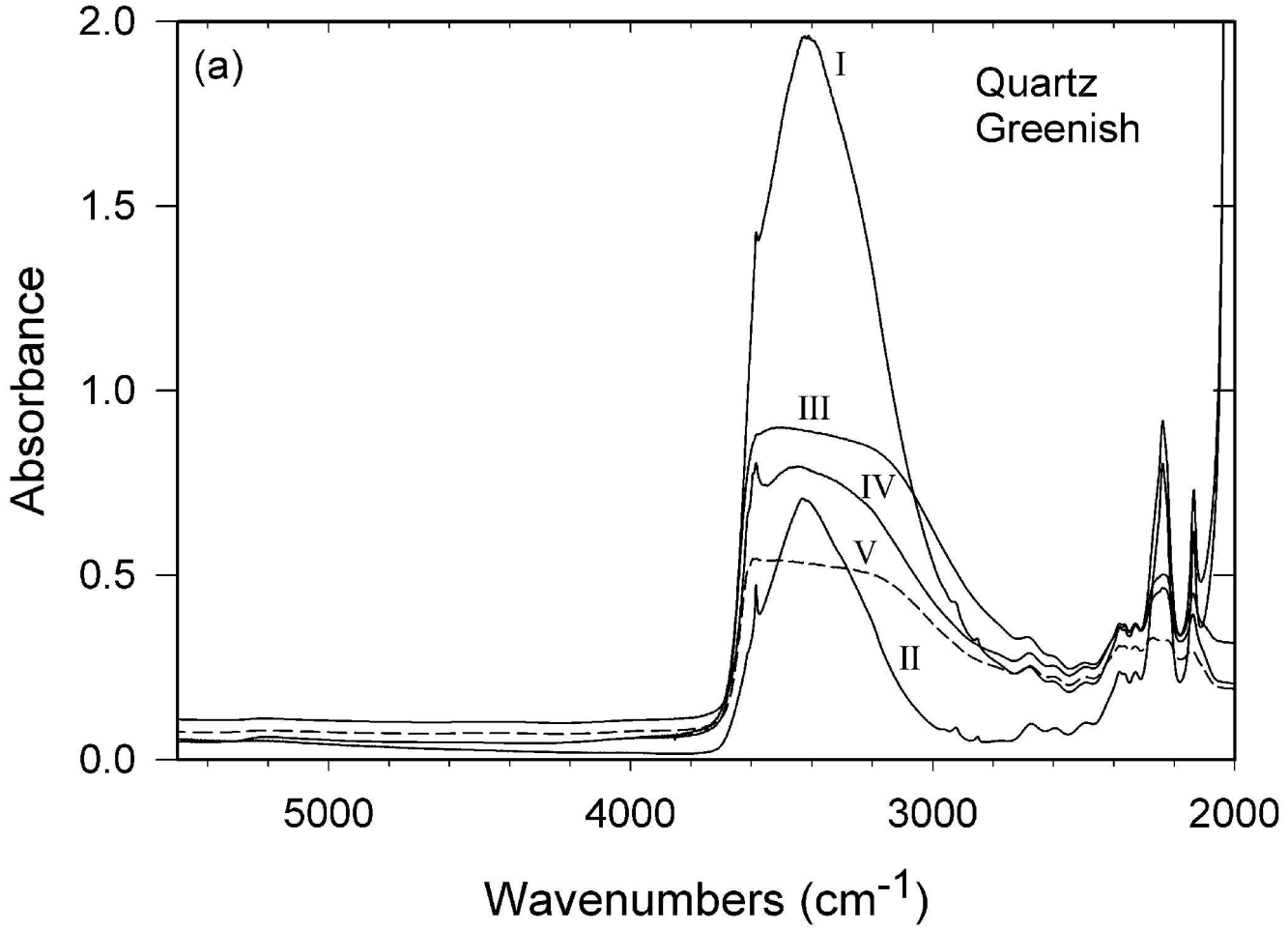
(a)
Quartz
Greenish
I
II
III
IV
V
Absorbance
2.0
1.5
1.0
0.5
0.0
5000
4000
3000
2000
Wavenumbers (cm-1)

Figure 9.

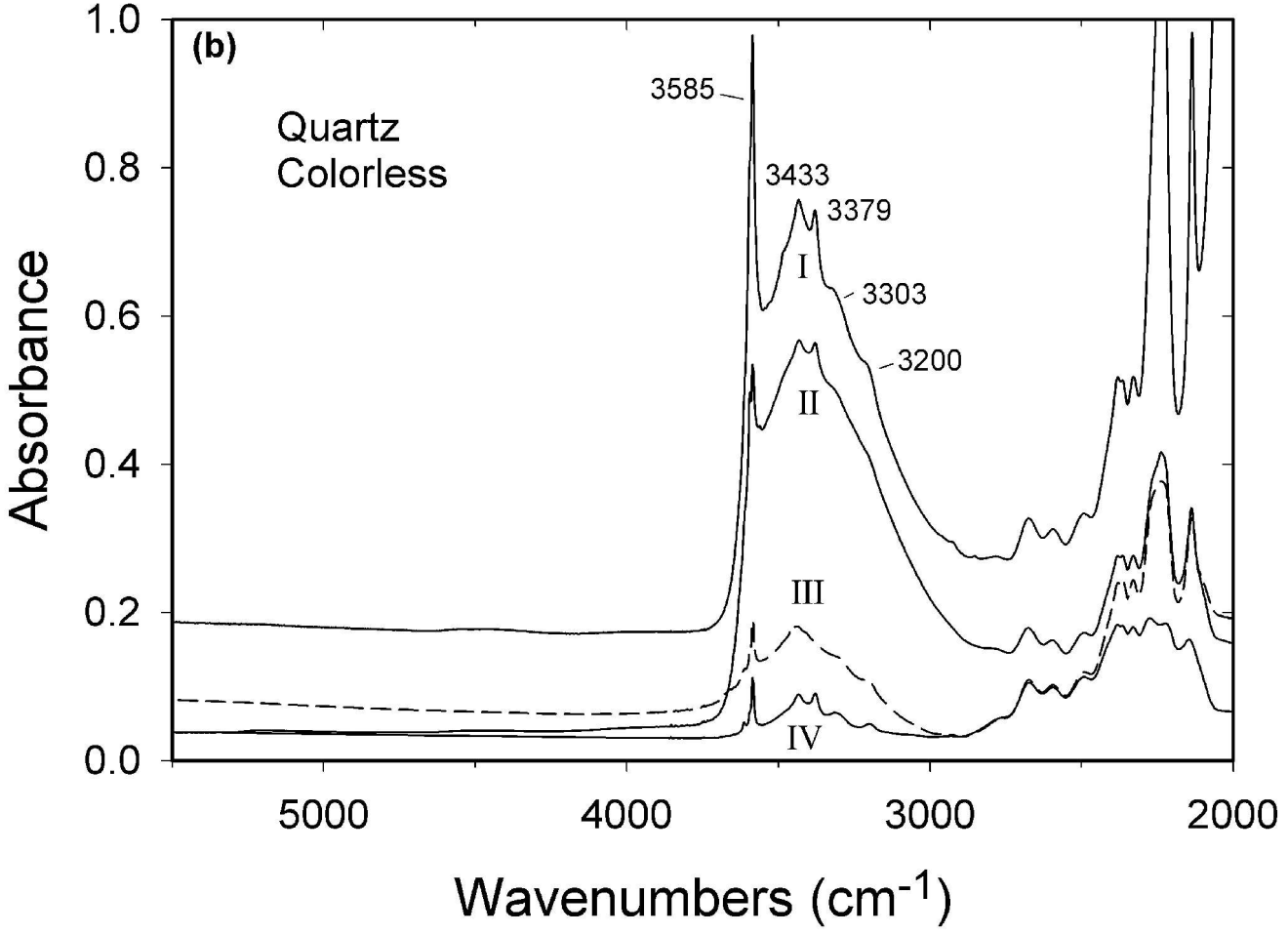
(b)
Quartz
Colorless
3585
3433
3379
3303
3200
I
II
III
IV
Absorbance
1.0
0.8
0.6
0.4
0.2
0.0
5000
4000
3000
2000
Wavenumbers (cm-1)

Table 1: LA-ICP-MS analysis results for TBAMP samples

Sample	original color	^{9}Be	^{11}B	^{23}Na	^{44}Ca	^{27}Al	^{39}K	^{7}Li	^{33}S	^{69}Ga	Position in sequence
003-1	dark amethyst	7	-	-	4166	-	14	2	29	3	top
006-BI	bicolored amethyst	-	-	-	1464	-	-	32	11	15	
006-BI	bicolored greenish gray	-	-	-	-	275	-	22	35	15	
006-C3	colorless	-	-	-	-	262	-	24	35	4	
006-G1	greenish gray	-	-	-	-	187	63	6	22	9	bottom
001-1	yellowish green	-	-	-	-	-	12	-	25	11	detrital
002-1	dark green	-	0.8	38	3987	218	-	8	27	15	detrital

- indicates levels below detection

Table 2: Summary of heating and radiation experiment results for TBAMP samples

Sample	original color	after heating	after irradiation of heated	after irradiation of original	position in sequence
003	dark purple amethyst	citrine	original amethyst color superimposed over citrine		top
006	bicolored amethyst	pale yellow	original amethyst color	no change	
006	bicolored grayish green	pale yellow	original grayish green		
006-base-2	bicolored greenish gray	turbid, colorless			
006-C	colorless	opaque white	dark smoky greenish purple	color on *r* and *z* sectors alternates between brownish and pale purple (24 hour exposure, darkening with additional exposure)	
006-G	greenish gray	turbid, colorless	dark brownish gray	dark brownish gray, smoky color (48 hour exposure) with slight purple overtones (72 hour exposure)	bottom
No number	pale purple amethyst	colorless	original pale purple		detrital
001	yellowish-green	citrine	brownish with purple overtones	no change (30 day exposure)	detrital
002	dark green	dark citrine	brownish with purple overtones		detrital